02,05

Coexistence of superconductivity and ferromagnetism in a nanocomposite based on porous glass with nickel and indium inclusions

© M.V. Likholetova[1], E.V. Charnaya[1], Yu.A. Kumzerov[2], A.V. Fokin[2], N.R. Grigorieva[1], V.M. Mikushev[1], E.V. Shevchenko[1]

[1] St. Petersburg State University,
St. Petersburg, Russia
[2] Ioffe Institute,
St. Petersburg, Russia

E-mail: e.charnaya@spbu.ru

Received August 9, 2023
Revised August 9, 2023
Accepted August 18, 2023

A nanocomposite was made based on a porous glass with nickel and indium embedded into pores. Mean pore size was equal to 4.8 nm according to nitrogen porosimetry. Dc magnetization was measured within the temperature range 1.8 to 400 K and field range −70 to 70 kOe. The superconducting transition was observed at a temperature of 3.405 K in the field 10 Oe. Bifurcation of the magnetization curves obtained under the ZFC and FC protocols and hysteresis loops of magnetization above the superconducting temperature evidence ferromagnetic ordering. Shifts of the magnetization isotherms within the superconducting phase were found, which depended on the field change direction. The shift signs show the impact of the inverse and/or electromagnetic proximity effects.

Keywords: superconductivity, ferromagnetism, magnetization, proximity effects, nanocomposite.

DOI: 10.61011/PSS.2023.10.57212.177

1. Introduction

Superconductivity and ferromagnetism are antagonists. In the superconducting state, the spins of Cooper pairs are antiparallel, while the exchange interaction in ferromagnets tends to order the spins in one direction. Despite these opposing trends, superconductivity and ferromagnetism can coexist in nanoheterogeneous structures [1–3]. Currently, the unique properties of superconductor-ferromagnet heterostructures are receiving much attention both from the point of view of fundamental physics and in terms of possible practical applications. Superconducting correlations can be induced in ferromagnetic regions due to the proximity effect, like in a normal metal. As a result, features of the heterostructures behavior arise, such as a nonmonotonic dependence of the superconducting transition temperature on the geometric parameters of ferromagnetic layers [4] and phase change to π in the superconductor-ferromagnet-superconductor layer structure [5]. A switching between two values of the critical current was observed, associated with ferromagnetic stray fields in superconducting magnetic structures [6,7]. Analysis of the spin-triplet state of the superconducting pair of electrons in superconductor-ferromagnet hybrid structures resulted in the emergence of a new field of superconducting spintronics [8,9].

A relatively less regular, but having a macroscopic total volume, hybrid structure containing superconducting and ferromagnetic nanoelements can be obtained by introducing small particles into nanoporous matrices. Due to the integral response of a large number of elements, the hybrid structure based on the porous matrix shall have high stability of characteristics. The superconductivity of porous silicate matrices (synthetic opals and porous glasses) with introduced nanoparticles of a number of low-melting metals was studied earlier, for example, in [10–16]. It was shown that such nanocomposites exhibit the properties of type II dirty superconductors with an upper critical field that is by several orders of magnitude higher than the critical field for the corresponding bulk metals. Strong pinning of vortices is due to their securing on structural inhomogeneities, accompanied by surface barriers overcoming. Features of critical lines in the phase diagrams of composite superconductors, which have a positive curvature in the temperature range below the superconducting transition, were noted. Thermomagnetic instabilities caused by avalanche-like processes in the vortex system were also observed. On the other hand, superconducting nanocomposites based on porous matrices filled with metals can be represented as a set of a large number of Josephson junctions [17]. The introduction into pores of particles of ferromagnetic materials, along with metals, shall lead to the formation of a large area of interphase boundaries and affect the superconducting properties due to proximity effects.

This paper presents the results of studies of the magnetic properties of nanocomposite, which is a porous silica glass with nickel and indium embedded in the pores.

2. Samples and experiment

Porous glass obtained as a result of segregation in sodium-borosilicate glass and subsequent leaching of the phase enriched in sodium and boron was used as a matrix [18]. Pore size was determined by nitrogen porosimetry using Quadrasorb SI. The average pore diameter was 4.8 nm.

Nickel nanoparticles were synthesized in pores as follows. At the first stage, the porous glass was filled with a melt of nickel nitrate heptohydrate, heated to 130°C to remove water and slowly heated to temperature of 400°C, which led to the decomposition of nickel nitrate with the formation of Ni_2O_3 and the nitrogen dioxide release. Then the porous glass with nickel oxide was placed in a steel ampoule, through which hydrogen was supplied at temperature of 600°C for 8 hours. As a result of the reaction of nickel oxide with hydrogen a metallic nickel and water were formed, which evaporated. The volume of nickel particles was monitored by the weight of the sample and amounted to about 10% of the total pore volume. X-ray powder diffraction confirmed the nickel formation in the pores.

Indium in a molten state was introduced into the remaining unfilled volume of the porous space under a pressure of up to 10 kbar. Indium crystallized in the pores upon cooling, which was confirmed by X-ray diffraction patterns at room temperature. For measurements, a sample was cut out in the form of a thin slab weighing 82.65 mg.

The dc magnetization was measured using a Quantum Design MPMS 3 SQUID magnetometer. Temperature range of measurements was 1.8–400 K. The dependences of magnetization on temperature in various applied magnetic fields were obtained in the sample heating mode after preliminary cooling to 1.8 K in a zero external field (zero field cooled mode, ZFC) and during subsequent cooling in field (field cooling mode, FC). Isotherms of field dependences of magnetization were taken in the field range from −70 to 70 kOe. The surfaces of the plate were oriented parallel to the external magnetic field.

3. Results and discussion

Temperature dependences of magnetization demonstrated bifurcation of ZFC and FC curves, indicating the presence of weak ferromagnetism in the sample under study, a slight increase in ZFC and FC curves with temperature decreasing, associated with the paramagnetic effect, and a transition to the superconducting state. An example of changes in magnetization in the applied field of 200 Oe is shown in Figure 1. (For color Figures see the electronic version of the journal).

The insert in Figure 1 shows the zoomed up curves, where the divergence between ZFC and FC dependences is better visible. Magnetization anomalies between 40 and 70 K are caused by the molecular oxygen presence. The magnetization in the temperature region below 4.3 K, measured when field of 10 Oe is applied in ZFC and FC modes, is shown in Figure 2. The superconducting transition is visible at temperature of $T_c = 3.405 \pm 0.015$ K, within the error coinciding with the superconductivity temperature of pure metallic indium (3.414 K).

Figure 2 shows that when approaching the lower limit of the temperature range of the experimental setup, the

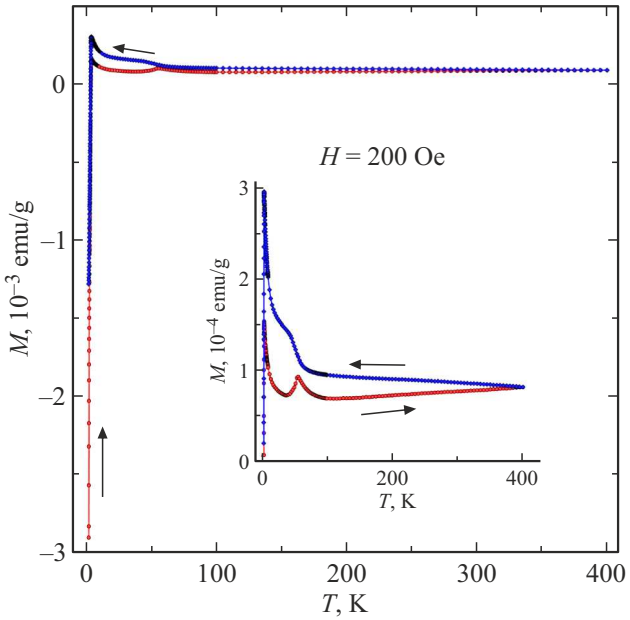

Figure 1. ZFC (red circles) and FC (blue diamonds) magnetizations vs. temperature in magnetic field of 200 Oe. The insert shows a zoomed up section of the graph. The arrows show the direction of temperature change.

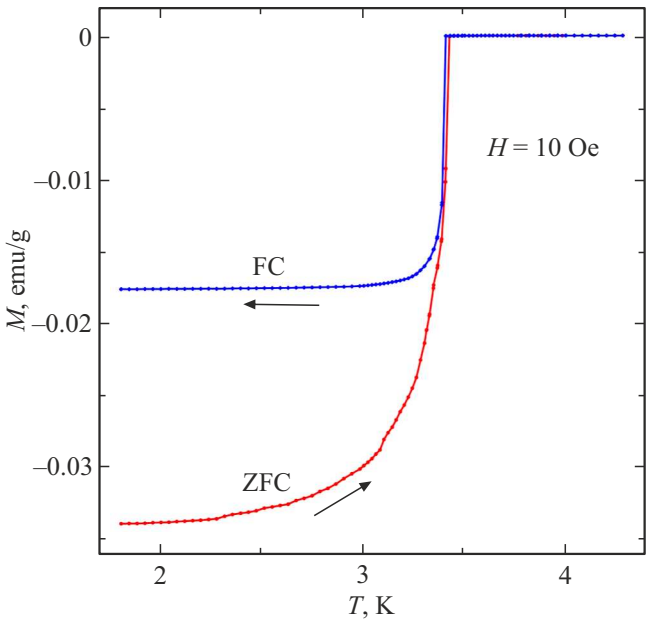

Figure 2. ZFC (red circles) and FC (blue diamonds) magnetizations vs. temperature in magnetic field of 10 Oe at low temperatures. The arrows show the direction of temperature change.

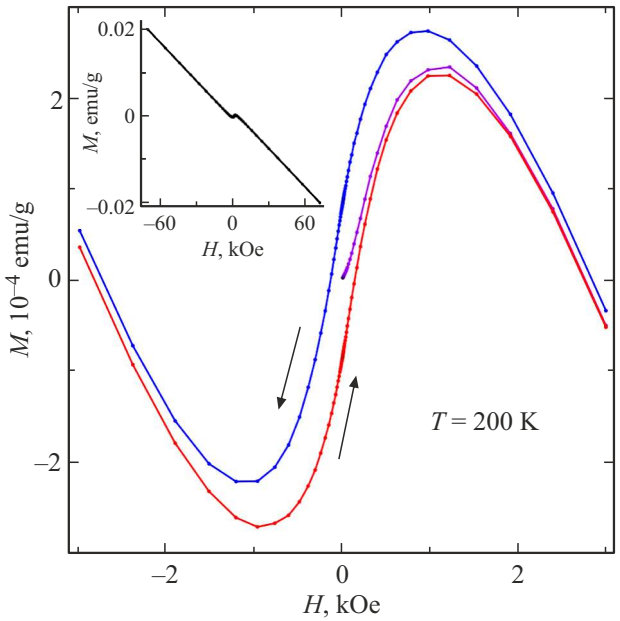

Figure 3. Isotherms of virgin (purple symbols), secondary (blue symbols) and tertiary (red symbols) magnetization in low-field region at temperature of 200 K. The arrows show the direction of field change. The insert shows complete dependence $M(H)$.

magnetization curves almost reach a plateau. The maximum shielding value in the ZFC mode reaches a significant value, close to shielding in a solid superconductor. In FC mode the magnetization modulus near 1.8 K is about two times lower than the magnetization modulus obtained in ZFC mode, which indicates weak pinning, in contrast to previously published results for nanocomposites with metal nanoparticles only in the pores [11–17].

Magnetization isotherms $M(H)$ were taken with an increase in the magnetic field from 0 to 70 kOe and a subsequent change in the field to −70 kOe and an increase to 70 kOe. Above the superconductivity temperature the hysteresis loops typical for ferromagnetic materials appear on the magnetization isotherms. As an example, Figure 3 shows the central part of the isotherm obtained in weak fields at temperature of 200 K. The complete curve $M(H)$ is shown in the insert to Figure 3.

It can be seen that at 200 K the main contributions to the magnetic properties of the nanocomposite are made by the matrix diamagnetism and the ferromagnetism of nickel in the pores. It should be emphasized that the hysteretic behavior of magnetization indicates that nickel in the pores does not transform into superparamagnetic state, despite the small size of the pores. This situation may arise because the nickel synthesis method described above does not lead to the formation of individual small particles of metallic nickel, but to the formation of a dendrite-like morphology, for example, when nickel crystallizes on the walls of pores. This assumption agrees with the bifurcation of ZFC and FC curves (Figure 1) and the absence of maxima in ZFC curves, which appear at the blocking temperature of superparamagnetic particles. In this case, the sizes of single-crystallinity of dendritic clusters significantly exceed the sizes of pores, since the broadening of peaks in X-ray diffraction patterns is comparable to instrumental broadening. Estimates for for the coercitivity and the fields at which the hysteresis loops close, give values slightly higher than the corresponding values for hollow nickel microspheres [19].

The example of hysteresis loops in the superconducting state is shown in Figure 4 for temperature of 2 K. If we do not take into account the shifts of the branches along the horizontal axis, the hysteresis shape has a form characteristic for type II superconductors with weak pinning.

The shown displacement of the secondary and tertiary branches of magnetization, obtained by decreasing and increasing the field, respectively, relative to each other and relative to the primary magnetization attract attention. The secondary branch of magnetization shifts towards higher fields, and the tertiary branch of magnetization shifts towards negative fields. As we know, there are no reports of such observations in the publications. However, recently, shifts in the maximum of critical currents registered in heterostructures containing layers of superconductor and ferromagnet were actively discussed [2,20,21]. Since for the set of Josephson junctions, which simulates the nanocomposite based on the porous matrix with inclusions of superconducting metals [17], the critical current is proportional to the difference between the secondary and tertiary magnetizations, then to interpret the behavior, the example of which is shown in Figure 4, it is possible

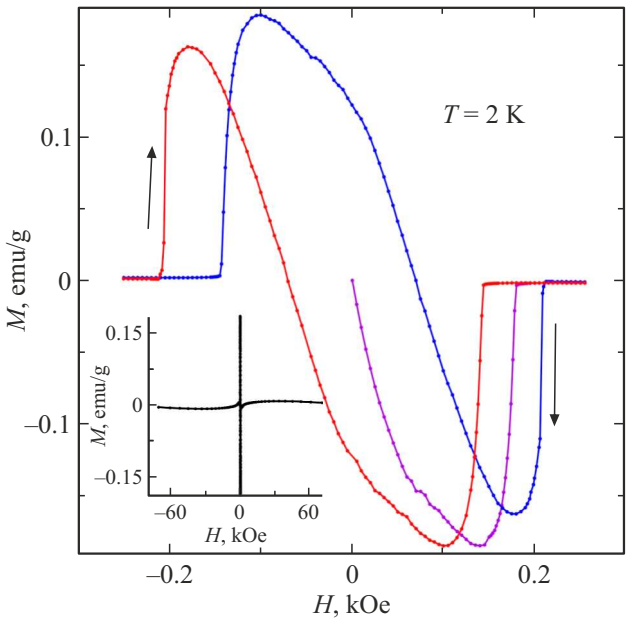

Figure 4. Isotherms of primary (purple symbols), secondary (blue symbols) and tertiary (red symbols) magnetization in low-field region at temperature of 2 K. The arrows show the direction of field change. The insert shows complete dependence $M(H)$.

apply theoretical models proposed to explain the shifts of Fraunhofer oscillations of the critical current. The direction of shift of the maximum critical current can be different, depending on the dominant shift mechanism. The most obvious is the influence of ferromagnetic stray fields [22]. In this case, the maximum of critical current observed when the magnetic field decreases from positive values to negative values shall be shifted towards negative fields due to the positive residual magnetization in the ferromagnet. Similarly, as the field increases, the current maximum shifts towards higher fields. The opposite sign of the shift is caused by the inverse proximity effect [23–26] and the electromagnetic proximity effect [27,28]. The inverse proximity effect is associated with the polarization of Cooper electron spins. The longer-range electromagnetic proximity effect is due to the excitation of superconducting currents in ferromagnet due to the proximity effect and the compensating currents appearance in the superconductor. It is shown in the paper [2] that depending on the geometric parameters of heterostructures both signs of the shift of Fraunhofer oscillations can be realized. The experimental results in Figure 4 demonstrate that for the nanocomposite with nickel and indium in pores the inverse and/or electromagnetic proximity effect dominates.

As it was suggested in the paper [2], the influence of inverse and electromagnetic proximity effects can lead to increase in the diamagnetic response from the heterostructure with superconducting and ferromagnetic layers. This may be related to the significant diamagnetic shielding in the nanocomposite under study (Figure 2).

Hysteresis loops in the temperature region of superconductivity of the nanocomposite make it possible to determine the values of the critical fields. At $T = 2\,\mathrm{K}$ the critical field along the primary branch of magnetization is approximately equal to 179 Oe, which practically coincides with the critical field for pure indium (177 Oe) [29]. This result differs considerably from the critical fields for porous matrices filled only with indium [12–14]. Namely, the upper critical field in the limit of zero temperature for opal with indium exceeded 3 kOe, and for porous glass filled with indium it exceeded 30 kOe.

4. Conclusion

The prepared nanocomposite based on porous silica glass with the average pore size of 4.8 nm with nickel and indium introduced into the pores demonstrated the coexistence of superconductivity with the transition temperature $3.405 \pm 0.015\,\mathrm{K}$ and ferromagnetism. The magnetic properties of the nanocomposite in the superconducting phase agree with the behavior of type II superconductors with weak pinning. Shifts of the magnetization branches on the isotherms $M(H)$ are discovered, their direction depends on the direction of the field change. The signs of the shifts are consistent with theoretical models of inverse and electromagnetic proximity effects.

Funding

The studies were funded by Russian Scientific Foundation, grant 21-72-20038. The measurements were carried out on the equipment of the Resource Centers of the Science Park of St. Petersburg State University.

Conflict of interest

The authors declare that they have no conflict of interest.

References

[1] A.I. Buzdin. Rev. Mod. Phys. **77**, 935 (2005).
[2] R. Satariano, L. Parlato, A. Vettoliere, R. Caruso, H.G. Ahmad, A. Miano, L. Di Palma, D. Salvoni, D. Montemurro, C. Granata, G. Lamura, F. Tafuri, G.P. Pepe, D. Massarotti, G. Ausanio. Phys. Rev. B **103**, 224521 (2021).
[3] R. Fermin, D. van Dinter, M. Hubert, B. Woltjes, M. Silaev, J. Aarts, K. Lahabi. Nano Lett. **22**, 2209 (2022).
[4] J.S. Jiang, D. Davidovic, D.H. Reich, C.L. Chien. Phys. Rev. Lett. **74**, 314 (1995).
[5] V.V. Ryazanov, V.A. Oboznov, A.Y. Rusanov, A.V. Veretennikov, A.A. Golubov, J. Aarts. Phys. Rev. Lett. **86**, 2427 (2001).
[6] R. Held, J. Xu, A. Schmehl, C.W. Schneider, J. Mannhart, M.R. Beasley. Appl. Phys. Lett. **89**, 163509 (2006).
[7] A.Y. Aladyshkin, A.A. Fraerman, S.A. Gusev, A.Y. Klimov, Y.N. Nozdrin, G.L. Pakhomov, V.V. Rogov, S.N. Vdovichev. J. Magn. Magn. Mater. **258–259**, 406 (2003).
[8] F.S. Bergeret, A.F. Volkov, K.B. Efetov. Rev. Mod. Phys. **77**, 1321 (2005).
[9] M. Eschrig. Rep. Prog. Phys. **78**, 104501 (2015).
[10] J.H.P. Watson. Phys. Rev. **148**, 223 (1966).
[11] C. Tien, A.L. Pirozerskii, E.V. Charnaya, D.Y. Xing, Y.S. Ciou, M.K. Lee, Yu.A. Kumzerov. J. Appl. Phys. **109**, 053905 (2011).
[12] E.V. Charnaya, C. Tien, M.K. Lee, Yu.A. Kumzerov. Properties of indium, gallium, and Ga-In alloys in confined geometry. In Indium: Properties,Technological Applications and Health Issues. Nova Sci., N.Y. (2013). P. 1–51.
[13] C. Tien, C.S. Wur, K.J. Lin, E.V. Charnaya, Yu.A. Kumzerov. Phys. Rev. B **61**, 14833 (2000).
[14] M.K. Lee, E.V. Charnaya, S. Mühlbauer, U. Jeng, L.J. Chang, Yu.A. Kumzerov. Sci. Rep. **11**, 4807 (2021).
[15] M.K. Lee, E.V. Charnaya, C. Tien, L.J. Chang, Yu.A. Kumzerov. J. Appl. Phys. **113**, 113903 (2013).
[16] E.V. Charnaya, C. Tien, M. K. Lee, Yu.A. Kumzerov. J. Phys.: Condens. Matter **21**, 455304 (2009).
[17] E.V. Charnaya, C. Tien, C.S. Wur, Yu.A. Kumzerov. Physica C **269**, 313 (1996).
[18] Dvukhfaznye stekla: struktura, svojstva, primenenie / Otv. red. B.G. Varshal. Nauka, L., (1991). (in Russian)
[19] Y. Wang, Q. Zhu, H. Zhang. J. Mater. Chem. **16**, 1212 (2006).
[20] L. Parlato, R. Caruso, A. Vettoliere, R. Satariano, H.G. Ahmad, A. Miano, D. Montemurro, D. Salvoni, G. Ausanio, F. Tafuri, G.P. Pepe, D. Massarotti, C. Granata. J. Appl. Phys. **127**, 193901 (2020).
[21] O.M. Kapran, T. Golod, A. Iovan, A.S. Sidorenko, A.A. Golubov, V.M. Krasnov. Phys. Rev. B **103**, 094509 (2021).

[22] A.Yu. Aladyshkin, A.V. Silhanek, W. Gillijns, V.V. Moshchalkov. Supercond. Sci. Tech. **22**, 053001 (2009).
[23] V.N. Krivoruchko, E.A. Koshina. Phys. Rev. B **66**, 014521 (2002).
[24] F.S. Bergeret, A.F. Volkov, K.B. Efetov. Phys. Rev. B **69**, 174504 (2004).
[25] F.S. Bergeret, A. Levy Yeyati, A. Martín-Rodero. Phys. Rev. B **72**, 064524 (2005).
[26] T. Löfwander, T. Champel, J. Durst, M. Eschrig. Phys. Rev. Lett. **95**, 187003 (2005).
[27] S.V. Mironov, A.S. Mel'nikov, A.I. Buzdin. Appl. Phys. Lett. **113**, 022601 (2018).
[28] Z. Devizorova, S.V. Mironov, A.S. Mel'nikov, A. Buzdin. Phys. Rev. B **99**, 104519 (2019).
[29] R.W. Shaw, D.E. Mapother, D.C. Hopkins. Phys. Rev. **120**, 88 (1960).

Translated by I.Mazurov